

## Cotransport of clay colloids and viruses in water saturated porous media

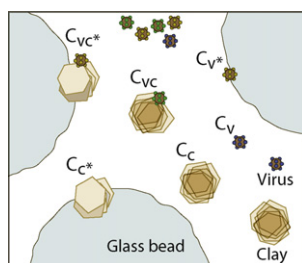
Vasiliki I. Syngouna, Constantin V. Chrysikopoulos\*

Environmental Engineering Laboratory, Department of Civil Engineering, University of Patras, Patras 26500, Greece

### HIGHLIGHTS

- ▶ Investigation of MS2 and  $\Phi$ X174 cotransport with clay colloids in porous media.
- ▶ The mass recovery of viruses and clay colloids decreased with decreasing  $U$ .
- ▶ The mass recovery of viruses decreased in the presence of clay colloids.
- ▶ Clay particles can facilitate or hinder virus transport in porous media.
- ▶ XDLVO is important only in the case of clay colloid attachment onto glass beads.

### GRAPHICAL ABSTRACT



### ARTICLE INFO

#### Article history:

Received 28 July 2012

Received in revised form 3 October 2012

Accepted 4 October 2012

Available online xxx

#### Keywords:

Viruses

$\Phi$ X174

MS2

Clay colloids

KGa-1b

STx-1b

Cotransport

### ABSTRACT

This study examines the cotransport of clay colloids and viruses in laboratory packed columns. Bacteriophages MS2 and  $\Phi$ X174 were used as model viruses, kaolinite (kGa-1b) and montmorillonite (STx-1b) as model clay colloids, and glass beads as model packing material. The combined and synergistic effects of clay colloids and pore water velocity on virus transport and retention in porous media were examined at three pore water velocities (0.38, 0.74, and 1.21 cm/min). The results indicated that the mass recovery of viruses and clay colloids decreased as the pore water velocity decreased; whereas, for the cotransport experiments no clear trend was observed. Temporal moments of the breakthrough concentrations suggested that the presence of clays significantly influenced virus transport and irreversible deposition onto glass beads. Mass recovery values for both viruses, calculated based on total virus concentration in the effluent, were reduced compared to those in the absence of clays. The transport of both suspended and attached onto suspended clay-particles viruses was retarded, compared to the tracer, only at the highest pore water velocity. Moreover both clay colloids were shown to hinder virus transport at the highest pore water velocity. At the lower velocities MS2 transport was hindered and  $\Phi$ X174 transport was facilitated with the exception of  $U=0.74$  cm/min in the presence of KGa-1b. Both MS2 and  $\Phi$ X174 were attached in greater amounts onto KGa-1b than STx-1b. Also, MS2 exhibited greater affinity than  $\Phi$ X174 for both clays.

© 2012 Elsevier B.V. All rights reserved.

### 1. Introduction

Suspended mobile colloids and particulate matter in the sub-surface environment can play a significant role as carriers of contaminants and biocolloids (e.g. bacteria and viruses). Numerous

experimental and theoretical studies have shown that, depending on the conditions of the physical system considered, colloids may facilitate or hinder the mobility of contaminants in porous and fractured formations [1–7]. Biocolloid transport mechanisms and sorption rates linked to various biological, chemical and physical factors have been well studied for individual species [8–11]. However, transport parameters obtained from studies performed with an individual colloid/biocolloid should not be generalized and applied to complex cotransport cases. Colloid facilitated virus

\* Corresponding author. Tel.: +30 2610 996531; fax: +30 2610 996573.

E-mail address: [gios@upatras.gr](mailto:gios@upatras.gr) (C.V. Chrysikopoulos).

**Nomenclature**

$A_{123}$	Hamaker constant of the interactive media, $ML^2/t^2$
$C_c$	suspended clay concentration, $M/L$
$C_{c0}$	clay initial concentration, $M/L$
$C_{c^*}$	concentration of clay particles attached onto glass beads, $M/M$
$C_{t0}$	tracer initial concentration, $M/L$
$C_{Total-v}$	total virus concentration, $M/L$
$C_v$	suspended virus concentration, $M/L$
$C_{v^*}$	concentration of viruses attached onto glass beads, $M/M$
$C_{vc}$	concentration of viruses attached onto suspended clay particles, $M/L$
$C_{vc^*}$	concentration of viruses attached onto clay particles previous attached onto glass beads, $M/M$
$C_{v0}$	virus initial concentration, $M/L$
$d_c$	average collector diameter, $L$
$d_p$	average colloidal particle diameter, $L$
$g$	acceleration due to gravity, $L/t^2$
$h$	separation distance between two approaching surfaces, $L$
$h_0$	minimum separation distance between two approaching surfaces, $L$
$i$	subscript indicating the various colloids or solute used in this study
$I_s$	ionic strength, mol/L
$k_B$	Boltzman's constant, $ML^2/(t^2 T)$
$L$	length of packed column, $L$
$M_n$	$n$ th normalized temporal moment, defined in Eq. (5), $t^n$
$M_{r(i)}$	mass recovery in the outflow of $i$
$M_{r(t)}$	tracer mass recovery in the outflow
$n$	subscript indicating the order of the moment
$r_p$	colloidal particle radius, $L$
RB	ratio of $M_{r(i)}$ , relative to $M_{r(t)}$
$t$	time, $t$
$T$	temperature in Kelvin, $T$
$U$	pore water velocity, $L/t$
$x$	Cartesian coordinate, $L$

**Greek letters**

$\alpha$	collision efficiency
$\alpha_{Total-v}$	apparent collision efficiency based on $C_{Total-v}$ in the effluent
$\alpha_v$	apparent collision efficiency based on $C_v$ in the effluent
$\beta_i$	contact angle of material $i$ , $^\circ$
$\eta_0$	dimensionless single-collector removal efficiency for favorable deposition
$\theta$	porosity
$\lambda_{AB}$	decay (Debye) length of water, $L$
$\mu_w$	absolute fluid viscosity, $M/(Lt)$
$\rho_b$	dry bulk density, $M/L^3$
$\rho_f$	fluid density, $M/L^3$
$\rho_p$	particle density, $M/L^3$
$\Phi_{AB}$	Lewis acid–base potential energy (J), $ML^2/t^2$
$\Phi_{AB(h=h_0)}$	Lewis acid–base free energy of interaction at $h = h_0$ ( $J/m^2$ ), $M/t^2$
$\Phi_{Born}$	Born potential energy (J), $ML^2/t^2$
$\Phi_{dl}$	double layer potential energy (J), $ML^2/t^2$
$\Phi_{max1}$	primary maximum of the total interaction energy (J), $ML^2/t^2$
$\Phi_{min1}$	primary minimum of total interaction energy (J), $ML^2/t^2$

$\Phi_{min2}$	secondary minimum of total interaction energy (J), $ML^2/t^2$ .
$\Phi_{vdW}$	van der Waals potential energy (J), $ML^2/t^2$ .

transport is expected to contribute to virus migration over greater distances than virus transport in the absence of colloids. Although considerable advances have been made on the prediction of colloid and biocolloid transport in porous and fractured media [12–22], and on biocolloid transport in the presence of other mobile colloids [23–28], better understanding of the physicochemical interactions between suspended clay colloids and viruses is clearly needed, as virus adsorption onto clays is not well understood, and different viruses appear to have different affinities for various clays, resulting in a variety of clay colloid-facilitated virus transport behaviors.

This paper focuses mainly on the effects of clay colloids on virus transport in water-saturated columns packed with glass beads. Bench scale experiments were performed to investigate the interactions between viruses and clays during their simultaneous transport (cotransport) in porous media. Centrifugation instead of the frequently employed filtration method was used for suspended-attached virus concentration separation. Also the synergistic effects of suspended clay colloids and pore water velocity on the attenuation and transport of viruses in porous media is examined. Furthermore, the surface properties of viruses, clays and glass beads were used to construct classical DLVO and extended-DLVO (XDLVO) potential energy profiles.

**2. Materials and methods****2.1. Bacteriophages and assay**

The bacteriophage MS2 (F-specific single-stranded RNA phage with effective particle diameter ranging from 24 to 26 nm) has been recommended as a surrogate for poliovirus due to similarities in size, and has been employed as a conservative tracer for enteric virus transport, because MS2 sorption onto the majority of soil types is low compared to many other viruses [29,30]. Also, similar removal rates for MS2, Hepatitis A virus, poliovirus 1, and echovirus 1 have been observed in columns packed with clay loam at pH range of 6–8 [31]. The bacteriophage  $\Phi X174$  (somatic single-stranded DNA phage with effective particle diameter ranging from 25 to 27 nm) has been recommended as a surrogate for norovirus due to similarities in size. Also, field studies conducted by DeBorde et al. [32] showed that  $\Phi X174$  was very stable and its inactivation was minimal over a period of half a year.  $\Phi X174$  under high hydrophobic conditions is considered the surrogate of choice compared with MS2 and PRD1, mainly due to its high stability and low hydrophobicity. Both bacteriophages are infecting *E. coli*, and were assayed by the double-layer overlay method [33], as outlined by Syngouna and Chrysikopoulos [34,35].

Coliphage concentrations have been reported to range widely in various polluted waters (e.g. in sewage waters may range from 10 to  $10^7$  PFU/mL [36]). Therefore, various virus concentrations, ranging from  $10^3$  to  $10^6$  PFU/mL were used in this study. Each concentration collected from the same virus stock solution was diluted with sterile distilled deionized water (ddH<sub>2</sub>O), which was purified with a Milli-Q UV plus water purification system containing a UV sterilization lamp (Millipore Corp., Massachusetts). For the separation of viruses adsorbed onto clay colloids from suspended viruses in the liquid phase, centrifugation instead of filtration [28] was used. After the addition of 0.3 mL of the density gradient separation reagent Histodenz (60% by weight, Axis-Shield PoC AS Company, Norway) to 2 mL of the liquid sample [37–39], the mixture was centrifuged at

2000 × g for 30 min so that the supernatant was free of clay colloids. In order to determine the efficiency of this method, the mixture in tubes were centrifuged for various time periods and it was observed that the time for the centrifugation of 30 min was optimal because the supernatant contained none of the clay colloids. Moreover, to assess whether Histodenz interfered with the virus concentration measurements, two sets of preliminary control experiments were conducted. In the first set, centrifuge tubes contained virus suspensions in ddH<sub>2</sub>O mixed with 0.3 mL of Histodenz solution. In the second set, centrifuge tubes contained only virus suspensions in ddH<sub>2</sub>O. Initial virus concentrations were measured for each control experiment. After centrifugation at 2000 × g for 30 min the supernatant contained all of the initial virus concentration in both sets of experiments.

The suspension of unattached viruses in the supernatant was pipetted out and the suspended viruses were determined. The absence of clay colloids in the supernatant was verified by a UV–vis spectrophotometer (UV-1100, Hitachi) at a wavelength of 280 nm. The concentration of attached viruses was determined by subtracting the mass of viruses that remained in suspension from the initial virus concentration in each sample. Because only viable viruses were measured in the water samples, it was important to exclude the effect of virus inactivation when evaluating interactions of viruses with clay colloids under the present experimental conditions. Previous batch inactivation experiments under identical experimental conditions (in the presence and absence of clays) suggested that no significant virus inactivation is expected during the experimental time period [40]. However, although the inactivation rates for the viruses used in this study are relatively small, MS2 inactivation was reported to be more than two times larger than that of ΦX174 [35]. Furthermore, the inactivation rate of MS2 was reported to be greater than that of ΦX174 in the presence of quartz sand under static and dynamic batch conditions at different temperatures [41]. Therefore, the difference in the inactivation rate coefficients is expected to lead to smaller MS2 breakthrough concentrations than ΦX174.

## 2.2. Clays

The clays used in this study were kaolinite (KGa-1b, well-crystallized kaolin, from Washington County, Georgia) [42], and montmorillonite (STx-1b, Ca-rich montmorillonite, Gonzales County, TX), purchased from the Clay Minerals Society (Columbia, USA). KGa-1b has specific surface area (SSA) of 10.1 m<sup>2</sup>/g, as evaluated by the Brunauer–Emmet–Teller (BET) method, and cation exchange capacity (CEC) of 2.0 mequiv./100 g [43]. STx-1b has a SSA of 82.9 m<sup>2</sup>/g [44], and assuming that the characteristics of STx-1b are comparable to those of STx-1, which is the previous batch of montmorillonite from the same area, its CEC is 84.4 mequiv./100 g [43]. The <2 μm colloidal fraction, used in transport experiments, was separated by sedimentation [45] and was purified following the procedure described by Rong et al. [38]. It should be noted that the treated clays (purified colloidal fraction) are smaller than the untreated particles and thus is reasonable to assume that the treated clays are expected to have higher SSA values than the untreated particles. The hydrodynamic diameter of the clay colloids was measured by a zetasizer (Nano ZS90, Malvern Instruments) and was found to be equal to  $d_p = 842.85 \pm 125.85$  nm for KGa-1b, and  $d_p = 1187 \pm 380.81$  nm for STx-1b, resulting in a virus-to-clay particle size ratio in the range from 0.026 to 0.036 for KGa-1b particles and from 0.016 to 0.032 for STx-1b particles. The optical density of the clay colloids was analyzed at a wavelength of 280 nm by a UV–vis spectrophotometer, and the corresponding clay concentrations were determined by the procedures developed by Chrysikopoulos and Syngouna [40].

## 2.3. Electrokinetic measurements

The Zeta potentials of the bacteriophages and clays, measured at pH 7 in sterile ddH<sub>2</sub>O by the zetasizer, were  $-40.4 \pm 3.7$  mV for MS2,  $-31.78 \pm 1.25$  mV for ΦX174,  $-26.03 \pm 2.77$  mV for KGa-1b, and  $-20.5 \pm 0.8$  mV for STx-1b [40]. Also, the isoelectric point (IEP) of MS2, ΦX174, and KGa-1b in ddH<sub>2</sub>O were  $pH_{IEP} = 4.1, 4.4,$  and 2.1, respectively [40]. All zeta potential measurements were obtained in triplicates. Furthermore, the zeta potential of glass beads stored in ddH<sub>2</sub>O at pH 7 was determined to be  $-54.6 \pm 2.4$  mV. For soft particles as viruses, the electrical double layer is formed not only outside but also inside the surface charge layer, consequently the zeta potential becomes less important and for some cases, loses its physical meaning [46,47]. In this study, the electrokinetic zeta potentials were used instead of the surface potentials. Note that all experiments were performed with sterile ddH<sub>2</sub>O (pH 7,  $I_s = 10^{-4}$  M), conditions that do not interfere with virus viability/inactivation [40], and the conventional DLVO and XDLVO interaction models were used, assuming that viruses behave as hard spheres.

## 2.4. Column experiments

All flow through experiments were conducted using a 30 cm long glass column with 2.5 cm diameter, which was packed with 2 mm diameter glass beads. Glass beads were used for the packing of the columns in order to eliminate possible experimental difficulties associated with real soil, which may provide numerous uncertainties that can considerably complicate the analysis of the experimental data. Note that this work is focused only on the interactions associated between clay colloids and viruses during cotransport. Certainly, further research is needed to fully understand the cotransport of clay colloids and viruses under field conditions.

Following the procedure previously described by Syngouna and Chrysikopoulos [35], the glass beads were soaked in concentrated 0.1 M HNO<sub>3</sub> (70%) for a 3 h time period to remove surface impurities. Next, the beads were rinsed with sterile ddH<sub>2</sub>O until the water conductivity, as determined by a conductivity meter, was negligible. Subsequently, the glass beads were soaked in 0.1 M NaOH for a 3 h time period, and rinsed repeatedly with ddH<sub>2</sub>O until the ionic strength ( $I_s$ ) of water was negligible ( $I_s = 10^{-4}$  M). The glass beads were dried in an oven at 105 °C, and then stored in screw cap sterile beakers until use in the column experiments. The column was packed with glass beads under standing ddH<sub>2</sub>O to minimize air entrapment. The estimated dry bulk density was estimated to be  $\rho_b = 1.61$  g/cm<sup>3</sup>, and the porosity  $\theta = 0.42$ . The column was placed horizontally to minimize gravity effects. A fresh column was packed for each experiment. Also, 3 pore volumes (PVs) of sterile ddH<sub>2</sub>O were passed through the column prior to each transport experiment. The entire packed column and glassware used for the experiments were sterilized in an autoclave at 121 °C for 20 min. Constant flow of ddH<sub>2</sub>O at three different flow rates of  $q = 2.5, 1.5$  and 0.8 ml/min, corresponding to pore water velocities of  $U = q/\theta = 1.21, 0.74,$  and 0.38 cm/min respectively, was maintained through the packed column with a peristaltic pump (Masterflex L/S, Cole-Palmer). One set of experiments was performed with viruses and clay colloids alone in order to determine their individual transport characteristics. Another set of cotransport experiments was performed to investigate the effect of the presence of clay colloids on virus transport. For each experiment, the clay colloidal suspension and the viral suspension were injected simultaneously into the packed column at the same flow rate for 3 PVs, followed by 3 PVs of ddH<sub>2</sub>O. All experiments were carried out at room temperature (~25 °C). Chloride, in the form of potassium chloride (KCl), was chosen as the nonreactive tracer for the transport experiments [48]. Effluent chloride concentrations

were measured using ion chromatography (ICS-1500, Dionex). All clay colloid transport experiments were repeated three times. For each cotransport experiment several measurements were made for each sample collected (before and after centrifugation). Only dilutions that resulted in the range of 20–300 plaques per plate were accepted for quantification, and each concentration measurement reported represents the average of two replicate plates.

### 3. Theoretical considerations

#### 3.1. Transport data analysis

Classical colloid filtration theory (CFT) was used to quantitatively compare the attachment of viruses onto glass beads and clay colloids. The dimensionless collision efficiency,  $\alpha$  (the ratio of the collisions resulting in attachment to the total number of collisions between suspended particles and collector grains), was calculated from each breakthrough curve [49]:

$$\alpha = -\frac{2d_c \ln(RB)}{3(1-\theta)\eta_0 L} \quad (1)$$

where  $d_c$  is the average collector diameter,  $\eta_0$  is the dimensionless single-collector removal efficiency for favorable deposition (in the absence of double layer interaction energy), and RB is the ratio of suspended particles mass recovery,  $M_{r(i)}$ , relative to the tracer mass recovery,  $M_{r(t)}$ , in the outflow:

$$RB = \frac{M_{r(i)}}{M_{r(t)}} \quad (2)$$

The mass recovery,  $M_r$ , of the tracer or the suspended particles was quantified by the following expression [50]:

$$M_r(L) = \frac{\int_0^\infty C_i(L, t) dt}{\int_0^{t_p} C_i(0, t) dt} \quad (3)$$

where  $L$  is the length of the packed column.

In this study, the suspended clay concentration was indicated by  $C_c$ . Also, for the cotransport experiments the total virus concentration,  $C_{\text{Total-v}}$ , was assumed to be equal to the effluent suspended virus concentration,  $C_v$ , plus the concentration of viruses attached onto suspended clay particles,  $C_{vc}$ :

$$C_{\text{Total-v}} = C_v + C_{vc} \quad (4)$$

The tracer, virus, and clay initial concentrations were denoted by  $C_{t0}$ ,  $C_{v0}$ , and  $C_{c0}$ , respectively; whereas, the concentration of clay particles attached onto glass beads is denoted by  $C_{c^*}$ . Using the concept of apparent collision efficiency introduced by Walshe et al. [28] two different apparent collision efficiencies were calculated. Worthy to note is that apparent collision efficiencies lump together several processes associated with virus attachment onto clay particles [28]. The first collision efficiency,  $\alpha_{\text{Total-v}}$ , is based on  $C_{\text{Total-v}}$  in the effluent and represents the attachment of  $C_v$  onto both glass beads and  $C_{c^*}$ . The second collision efficiency,  $\alpha_v$ , is based on  $C_v$  in the effluent and represents the attachment of both  $C_v$  and  $C_{vc}$  onto glass beads, denoted as  $C_{v^*}$  and  $C_{vc^*}$ , respectively, as well as the attachment of  $C_v$  onto both  $C_c$  and  $C_{c^*}$ , denoted as  $C_{vc}$  and  $C_{vc^*}$ , respectively (for notation clarification see Fig. 1).

The collision efficiencies,  $\alpha$ , for MS2 and  $\Phi$ X174 were calculated for the experimental conditions of this study using Eq. (1), where the  $\eta_0$  values were obtained from an existing correlation [51], with the following parameter values for the complex Hamaker constant of the interactive media (virus–water–glass beads/clay colloids–water–glass beads)  $A_{123} = 7.5 \times 10^{-21}$  ( $\text{kg m}^2/\text{s}^2$ ) [52], Boltzman constant  $k_B = 1.38 \times 10^{-23}$  ( $\text{kg m}^2/(\text{s}^2 \text{K})$ ), fluid absolute temperature  $T = 298 \text{ K}$ , particle diameter  $d_p = 2.5 \times 10^{-8}$  and  $2.6 \times 10^{-8} \text{ m}$  for MS2 and  $\Phi$ X174, respectively, particle density

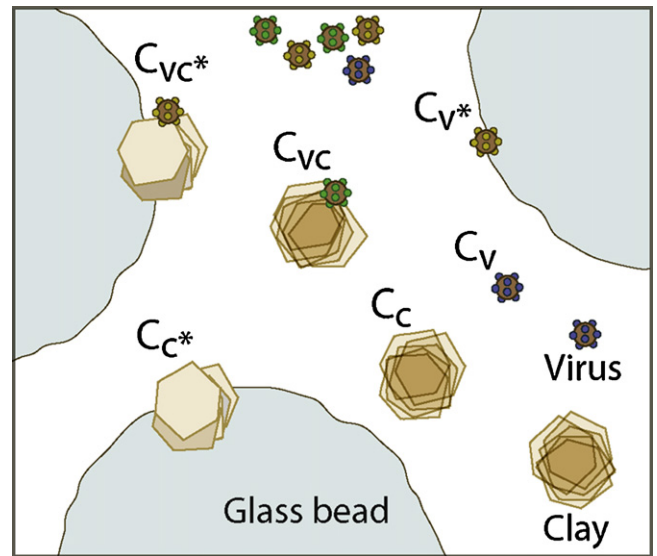


Fig. 1. Schematic illustration of the six concentration components involved in cotransport experiments of this study.

$\rho_p = 1420 \text{ kg/m}^3$  for MS2 [28],  $1600 \text{ kg/m}^3$  for  $\Phi$ X174 [53], and  $2650 \text{ kg/m}^3$  for clay colloids [54], fluid density  $\rho_f = 999.7 \text{ kg/m}^3$ , absolute fluid viscosity  $\mu_w = 8.91 \times 10^{-4} \text{ kg/(m s)}$ , and acceleration due to gravity  $g = 9.81 \text{ m/s}^2$ .

The concentration breakthrough data obtained at location  $x = L$  were analyzed by the normalized temporal moments, which are defined as [50]:

$$M_n(x) = \frac{\int_0^\infty t^n C_i(x, t) dt}{\int_0^\infty C_i(x, t) dt} \quad (5)$$

The first normalized temporal moment,  $M_1$ , characterizes the center of mass of the concentration breakthrough curve and defines the mean breakthrough time or average velocity. The second normalized temporal moment,  $M_2$ , characterizes the spreading of the breakthrough curve. Worthy to note is that the ratio  $M_{1(i)}/M_{1(t)}$  indicates the degree of velocity enhancement of colloid particle  $i$  relative to the conservative tracer. If this ratio is less than one, there exists colloid retardation, and if it is greater than one there exists velocity enhancement of colloid transport. In this study, four different  $M_{1(i)}/M_{1(t)}$  ratios were calculated based on the effluent concentrations:  $C_{\text{Total-v}}$ ,  $C_c$ ,  $C_v$ , and  $C_{vc}$ .

#### 3.2. DLVO and XDLVO calculations

The interaction energy between two approaching surfaces versus their separation distance typically consists of a primary minimum,  $\Phi_{\text{min}1}$  (deep energy “well”), a primary maximum,  $\Phi_{\text{max}1}$  (energy barrier to attachment and detachment), and the secondary minimum,  $\Phi_{\text{min}2}$  (shallow energy “well”). Classical and extended DLVO theories were employed for the evaluation of virus–glass and clay–glass beads interactions. The classical DLVO theory assumes that the total interaction energy,  $\Phi_{\text{DLVO}}$ , between two surfaces equals the arithmetic sum of the van der Waals,  $\Phi_{\text{vdw}}$ , double layer,  $\Phi_{\text{dl}}$ , and Born,  $\Phi_{\text{Born}}$ , potential energies [55]:

$$\Phi_{\text{DLVO}}(h) = \Phi_{\text{vdw}}(h) + \Phi_{\text{dl}}(h) + \Phi_{\text{Born}}(h) \quad (6)$$

where  $h$  [m] is the separation distance between the approaching surfaces. Whereas, the extended DLVO (XDLVO) theory assumes that the total interaction energy between surfaces is the sum of

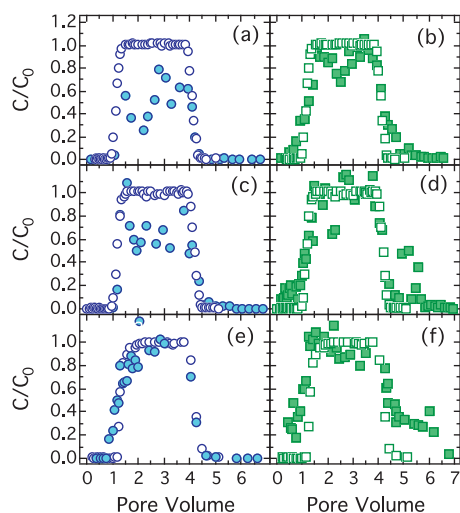


**Fig. 2.** Experimental data for transport of chloride tracer (open symbols), bacteriophages MS2 (filled circles), and  $\Phi$ X174 (filled squares) with  $U$  equal to: (a, b) 0.38; (c, d) 0.74; and (e, f) 1.21 cm/min.

$\Phi_{DLVO}$  and Lewis acid–base,  $\Phi_{AB}$ , interaction energies between two approaching surfaces [56]:

$$\Phi_{XDLVO}(h) = \Phi_{DLVO}(h) + \Phi_{AB}(h) \quad (7)$$

The Lewis acid–base interaction energy for the case of sphere–plate interactions can be calculated with the following relation [57,58]:

$$\Phi_{AB}(h) = 2\pi r_p \lambda_{AB} \Phi_{AB(h=h_0)} \exp\left[-\frac{h_0 - h}{\lambda_{AB}}\right] \quad (8)$$

where  $\Phi_{AB(h=h_0)}$  [J/m<sup>2</sup>] is the Lewis acid–base free energy of interaction between two surfaces at  $h = h_0$  (i.e., at “contact”),  $r_p$  is the particle radius,  $\lambda_{AB}$  [nm] is the decay (Debye) length of water, which has been reported to range from 0.4 to 32 nm [59]. For this work, it was assumed that  $\lambda_{AB} = 1$  nm [60], and  $h_0 = 0.25$  nm. Currently there are two methods that have been used for the estimation of  $\Phi_{AB(h=h_0)}$ : a theoretical approach developed by van Oss [57] and an empirical approach by Yoon et al. [59]. Bergendahl and Grasso [56] compared the two approaches and found that they gave similar results. In this study, the empirical approach developed by Yoon et al. [59] was employed, where the degree of hydrophobicity was determined using the following water contact angles:  $\beta_{MS2} = 33 \pm 1^\circ$ ,  $\beta_{\Phi X174} = 26 \pm 1.7^\circ$  [61],  $\beta_{KGa-1b} = 46.1^\circ$ ,  $\beta_{STx-1} = 20.5 \pm 2.8^\circ$  [62], and  $\beta_{glass} = 32 \pm 5^\circ$  [63]. It should be noted that the contact angles used in this study were obtained from published studies conducted under very similar experimental conditions following identical purification procedures to the work presented here.

## 4. Results and discussion

### 4.1. Transport experiments

Fig. 2 presents the normalized MS2 and  $\Phi$ X174 breakthrough data for three different interstitial velocities ( $U = 1.21, 0.74, 0.38$  cm/min), together with the normalized chloride breakthrough data. The corresponding  $M_r$  values, as calculated with Eq. (3), are listed in Table 1. The peak-concentrations and mass recoveries for both viruses increased with increasing  $U$ . With no exception, all estimated  $M_r$  values for MS2 were lower than those of  $\Phi$ X174. MS2 generally exhibits poorer attachment to solid surfaces [64], and  $\Phi$ X174 is less negatively charged than MS2 at the experimental conditions of this study. Therefore,  $\Phi$ X174 is expected to

attach onto the solid matrix more than MS2. On the contrary, our results indicate that more MS2 than  $\Phi$ X174 was retained in the packed column. Similar findings were reported by Syngouna and Chrysikopoulos [35], who conducted experiments in columns packed with sand using practically identical specific discharge. Only at the lower  $U$ ,  $\Phi$ X174 was retained slightly in the packed column. Although low  $M_r$  values cannot lead to the conclusion that MS2 particles retained were irreversibly attached or inactivated, the possibility that low  $M_r$  values are caused by irreversible attachment and inactivation cannot be excluded. Consequently, the observed low  $M_r$  values of MS2 may be attributed to the higher attachment and inactivation rates found for MS2 than  $\Phi$ X174 [35,41]. For the case of the lowest  $U$ , slight enhancement was observed ( $M_{1(i)}/M_{1(t)} > 1$ ) for both viruses, while only for the highest  $U$  the ratio  $M_{1(i)}/M_{1(t)} < 1$  (see Table 1), suggesting that the transport of MS2 was retarded by 13% compared to the tracer, and the transport of  $\Phi$ X174 was retarded by 5%.

Fig. 3 presents the normalized KGa-1b and STx-1b breakthrough data for the three interstitial velocities:  $U = 1.21, 0.74, 0.38$  cm/min. The ratio of the first normalized temporal moment of KGa-1b to that of  $Cl^-$  was computed for each breakthrough curve and the results are listed in Table 1. Note that  $M_{1(i)}/M_{1(t)} > 1$  for the two lower  $U$  values, indicating that KGa-1b was enhanced by 17–20%. Also, KGa-1b was significantly retained by the packed column, especially for the lowest  $U$ . Lower attachment of KGa-1b onto the glass beads was observed at the highest  $U$  (see Fig. 3) suggesting that hydrodynamics possibly had greater influence on the detachment than the attachment process. Similar results were reported by Vasiliadou and Chrysikopoulos [39], who conducted kaolinite transport experiments in saturated columns packed with glass beads and observed that kaolinite mass retention decreased with increasing  $U$ . For all cases examined in this study  $M_{1(i)}/M_{1(t)} > 1$  for STx-1b, indicating that STx-1b was enhanced by 1–25%. The  $M_r$  values, listed in Table 1, indicated that there was no significant effect of  $U$  on STx-1b retention by the packed column. Higher mass recoveries were observed for STx-1b than KGa-1b for the lowest  $U$ . The higher retention of KGa-1b could be attributed to its higher hydrophobicity [40]. However, other investigators have reported that Ca-montmorillonite tends to aggregate, whereas kaolinite remains dispersed, allowing the retention of an effective covering of hydrophobic surfaces and facilitating the absorption of water [65,66]. Note that Vasiliadou and Chrysikopoulos [39] found that although the attachment and detachment rate coefficients for kaolinite transport increased with

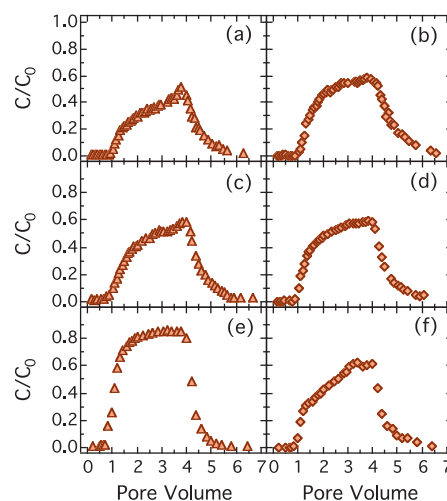


**Fig. 3.** Experimental data (symbols) for transport of KGa-1b (triangles), and STx-1b colloids (diamonds) with  $U$  equal to: (a, b) 0.38; (c, d) 0.74; and (e, f) 1.21 cm/min.

**Table 1**  
Data analysis for the transport and cotransport experiments.

Initial concentration $C_{t0}, C_{v0}, C_{c0}$	$U$ (cm/min)	$M_r$ (%) for $C_{Total-v}$ or $C_c$	$M_r$ (%) for $C_v$	$M_r$ (%) for $C_{vc}$	$M_{1(i)}/M_{1(t)}$ for $C_{Total-v}$ or $C_c$	$M_{1(i)}/M_{1(t)}$ for $C_v$	$M_{1(i)}/M_{1(t)}$ for $C_{vc}$	$\alpha_{Total-v}$	$\alpha_v$
<b>Transport experiments</b>									
Tracer $Cl^-$									
0.01 mol/L	1.21	100			1				
0.01 mol/L	0.74	100			1				
0.01 mol/L	0.38	94.9			1				
$\Phi X174$									
3185 PFU/mL	1.21	100			0.95			0.00026	
8867 PFU/mL	0.74	100			1.08			0.00018	
12,300 PFU/mL	0.38	96.2			1.06			0.0044	
MS2									
282,000 PFU/mL	1.21	74.2			0.87			0.075	
1350 PFU/mL	0.74	70.1			1.02			0.063	
6000 PFU/mL	0.38	49.7			1.09			0.077	
KGa-1b									
55.9 mg/L	1.21	87			0.9			0.116	
62.8 mg/L	0.74	53.5			1.17			0.312	
44.3 mg/L	0.38	39.8			1.2			0.229	
STx-1b									
101.0 mg/L	1.21	56.1			1.01			0.163	
100.1 mg/L	0.74	58.6			1.14			0.257	
119.0 mg/L	0.38	60.2			1.25			0.07	
<b>Cotransport experiments</b>									
$\Phi X174$ -KGa-1b									
12,367 PFU/mL	1.21	57	29.8	22.3	0.86	0.87	0.85	0.146	0.314
62.8 mg/L		21.3			1				
3238 PFU/mL	0.74	40.5	24.4	19.3	1.14	1.22	1.03	0.164	0.256
57.5 mg/L		30.3			1.2				
1418 PFU/mL	0.38	65.5	45.8	17.8	1.1	1.06	1.17	0.048	0.088
54.4 mg/L		13.9			1.12				
$\Phi X174$ -STx-1b									
84,800 PFU/mL	1.21	48.9	37.3	11.7	0.91	0.93	0.89	0.186	0.256
100.7 mg/L		36.2			0.96				
61,667 PFU/mL	0.74	47.5	39.3	8.2	1.1	1.07	1.25	0.135	0.17
78.5 mg/L		22.1			1.57				
40,000 PFU/mL	0.38	42.6	37.8	10.6	1.07	1.06	1.1	0.097	0.11
78.5 mg/L		31.2			1.29				
MS2-KGa-1b									
4738 PFU/mL	1.21	65.7	8.95	55.4	0.87	1.03	0.84	0.106	0.61
63.8 mg/L		52			0.83				
2425 PFU/mL	0.74	28.2	6.6	21.4	1.14	1.25	1.09	0.223	0.468
69.1 mg/L		51.9			1.03				
51,500 PFU/mL	0.38	76.8	50.09	26.3	1.14	1.16	1.09	0.029	0.074
62.8 mg/L		26			1.21				
MS2-STx-1b									
520,333 PFU/mL	1.21	35.4	24.6	10.8	0.83	0.84	0.8	0.261	0.353
87.7 mg/L		32.7			0.93				
181,333 PFU/mL	0.74	43.8	17.9	25.6	1.08	1.12	1.06	0.145	0.303
91.3 mg/L		48			1.1				
406,000 PFU/mL	0.38	47	33.1	13.9	1.13	1.16	1.04	0.083	0.121
115.4 mg/L		35.1			1.26				

increasing flow rate, the ratio of attachment to detachment rate coefficients decreased with increasing flow rate.

#### 4.2. Cotransport experiments

Fig. 4 presents the normalized  $\Phi X174$  and clay (KGa-1b, STx-1b) cotransport breakthrough data for three interstitial velocities:  $U = 1.21, 0.74, 0.38$  cm/min. The corresponding  $M_r$  values, based on  $C_{Total-v}$  of  $\Phi X174$  in the effluent, as calculated with Eq. (3), were considerably reduced in the presence of clay colloids compared to those obtained in the absence of them (see Table 1). This suggested that some clay-bound viruses were retained in the column due to clay attachment onto glass beads [37,39]. Furthermore, the ratios  $M_{1(i)}/M_{1(t)}$ , based on  $C_{Total-v}$  of  $\Phi X174$  (see Table 1) indicated that the transport of  $C_{Total-v}$  for  $\Phi X174$  was retarded (9–14%) only at the highest  $U$  compared to the tracer, and STx-1b was retarded 4% only at the highest  $U$ . Also, KGa-1b was enhanced (0–12%) in all cases examined for  $\Phi X174$  and KGa-1b cotransport. Moreover,

$M_{1(i)}/M_{1(t)}$  ratios, based on  $C_v$  of  $\Phi X174$ , indicated that the transport of  $C_v$  was retarded 13% in the presence of KGa-1b, and 7% in the presence of STx-1b compared to the tracer only at the highest  $U$ . The same trend was observed for  $M_{1(i)}/M_{1(t)}$  ratios based on  $C_{vc}$  of  $\Phi X174$ . It is clear (see Table 1) that at the highest  $U$ , clay colloids hindered the transport of  $\Phi X174$  ( $M_{1(i)}/M_{1(t)}$  of  $C_{vc} < M_{1(i)}/M_{1(t)}$  of  $C_{Total-v} < M_{1(i)}/M_{1(t)}$  of  $C_v < 1$ ). Worthy to note is that, except for the case of  $U = 0.74$  cm/min in the presence of KGa-1b,  $C_{vc}$  of  $\Phi X174$  was enhanced more than  $C_{Total-v}$  of  $\Phi X174$ . Both clay colloids facilitate  $\Phi X174$  transport ( $M_{1(i)}/M_{1(t)}$  of  $C_{vc} > M_{1(i)}/M_{1(t)}$  of  $C_{Total-v} > M_{1(i)}/M_{1(t)}$  of  $C_v > 1$ ) at the lowest  $U$  (see Table 1).

Fig. 5 shows the normalized MS2 and clay (KGa-1b, STx-1b) cotransport breakthrough data for three interstitial velocities:  $U = 1.21, 0.74, 0.38$  cm/min. The various  $M_{1(i)}/M_{1(t)}$  ratios based on  $C_{Total-v}$  of MS2, listed in Table 1, indicated that  $C_{Total-v}$  of MS2 was retarded (13–17%) compared to the tracer only at the highest  $U$ . The same trend was observed at the highest  $U$  for  $M_{1(i)}/M_{1(t)}$  ratios based on  $C_v$  and  $C_{vc}$  of MS2, except when KGa-1b was present,

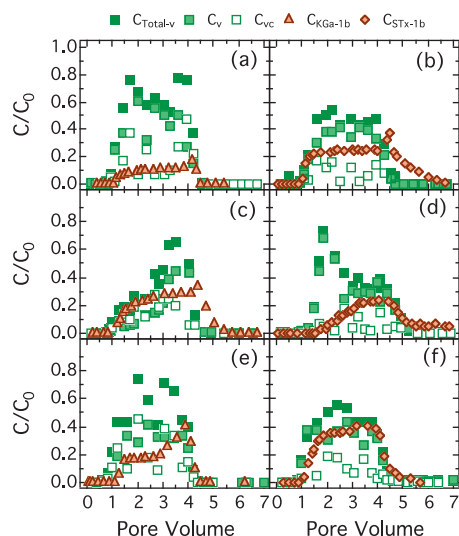


**Fig. 4.** Experimental data for cotransport of  $\Phi X174$  with KGa-1b (a, c, e), and STX-1b (b, d, f) with  $U$  equal to: (a, b) 0.38; (c, d) 0.74; and (e, f) 1.21 cm/min.

where slight enhancement for  $C_v$  of MS2 was observed. Also, KGa-1b was retarded 17% and STX-1b 7% compared to the tracer at  $U = 1.21$  cm/min. At the lowest  $U$ , all concentrations ( $C_{Total-v}$ ,  $C_v$ ,  $C_{vc}$ , and  $C_c$ ) were significantly enhanced compared to the tracer. Worthy to note is that for all cases examined,  $C_v$  of MS2 was enhanced more than  $C_{Total-v}$  of MS2, and  $C_{Total-v}$  of MS2 was enhanced more than  $C_{vc}$  of MS2 compared to the tracer for both clays employed (KGa-1b, STX-1b). Thus both clays hinder MS2 transport ( $M_{1(i)}/M_{1(t)}$  of  $C_{Total-v} > M_{1(i)}/M_{1(t)}$  of  $C_{vc} > 1$ ) at the lowest  $U$  (see Table 1). Therefore, depending on the physicochemical conditions, colloid particles can facilitate or hinder the transport of viruses in porous media.

The  $M_r$  values for  $\Phi X174$ , MS2, KGa-1b and STX-1b, as calculated with Eq. (3), for all three  $U$  examined, are listed in Table 1. Note that the  $M_r$  for both  $\Phi X174$  and MS2, based on  $C_{Total-v}$  equals the  $M_r$  based on  $C_v$  plus the  $M_r$  based on  $C_{vc}$ . With only exception the case for  $U = 0.38$  cm/min, all  $M_r$  values for MS2, calculated based on  $C_{Total-v}$  were reduced compared to those in the absence of clays.

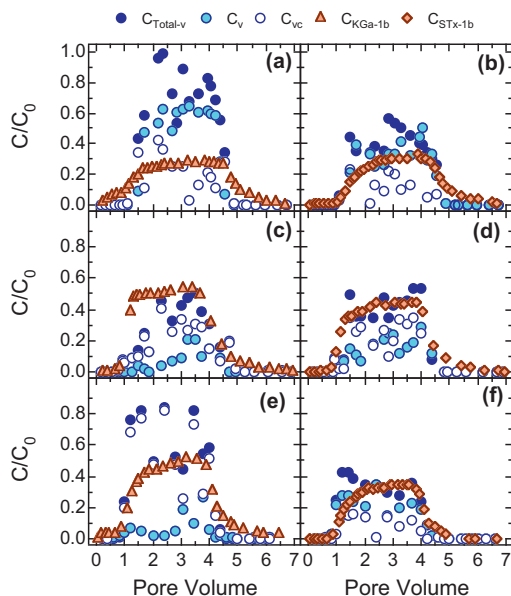


**Fig. 5.** Experimental data for cotransport of MS2 with KGa-1b (a, c, e), and STX-1b (b, d, f) with  $U$  equal to: (a, b) 0.38; (c, d) 0.74; and (e, f) 1.21 cm/min.

In the presence of KGa-1b, the  $M_r$  values based on  $C_{vc}$  of MS2 were quite high (21.4–55.4%). In the presence of STX-1b, the  $M_r$  values based on  $C_{Total-v}$  of MS2 were lower than those in the presence of KGa-1b. Furthermore, for  $\Phi X174$ , in the presence of KGa-1b, the various  $M_r$  values, listed in Table 1, indicated that by increasing  $U$ , the difference between  $C_{Total-v}$  and  $C_v$  of  $\Phi X174$  also increased, suggesting that more viruses were attaching onto suspended KGa-1b. This was reflected in the increased  $M_r$  based on  $C_{vc}$  of  $\Phi X174$  (17.8–22.3%). Whereas, in the presence of STX-1b, the  $M_r$  values based on  $C_{vc}$  of  $\Phi X174$  were considerably lower (8.2–11.7%). The possibility that the inactivation of  $C_v$  and  $C_{vc}$  is not identical should not be eliminated. However, it has been reported in the literature that the inactivation rate of  $C_v$  and  $C_{vc}$  in batch experiments is quite similar [34,35]. However, it has been reported in the literature that inactivation rates for  $C_v$  and  $C_{vc}$  are different [12,13,67–69]. Consequently, it is quite reasonable to assume that the inactivation rates for  $C_{vc}$  and  $C_{vc}^*$  are different. Also, the presence of viruses affected  $C_c$  transport because the  $M_r$  of both KGa-1b and STX-1b was substantially reduced in the presence of both viruses compared to the case of  $C_c$  transport in the absence of viruses (see Table 1). The  $M_r$  values for both KGa-1b and STX-1b based on  $C_c$  were lower in the presence of  $\Phi X174$ , but no significant differences were observed between the different  $U$  values (see Table 1). Moreover, similar  $M_r$  values based on  $C_c$  were observed for both KGa-1b and STX-1b in the presence of viruses at every  $U$  examined. The various  $M_r$  values for  $\Phi X174$ , MS2, KGa-1b and STX-1b are illustrated graphically in Fig. 6.

The collision efficiency values,  $\alpha_{Total-v}$ , based on  $C_{Total-v}$ , and  $\alpha_v$  values based on  $C_v$ , were calculated with Eq. (1) for all three  $U$ , and they are listed in Table 1. The  $\alpha_{Total-v}$  holds information about the adsorption of  $C_{Total-v}$  onto glass beads (transport experiments) and the adsorption of  $C_{Total-v}$  onto glass beads and  $C_c^*$  (cotransport experiments). The  $\alpha_{Total-v}$  values of MS2 in the transport experiments were higher than those of  $\Phi X174$  for all  $U$  (see Table 1). This was attributed to the more conservative adsorption behavior of  $\Phi X174$  than that of MS2, which is in agreement with previous results [35]. Moreover, in the presence of clay colloids (cotransport experiments),  $\alpha_{Total-v}$  values were higher for both viruses in all cases examined, which indicated that more attachment sites were available on the solid matrix (glass beads and  $C_c^*$ ). In the presence of STX-1b,  $\alpha_{Total-v}$  values decreased with decreasing  $U$ , while in the presence of KGa-1b no clear trend was observed. Furthermore, the relative high  $\alpha_v$  values ( $\alpha_v > \alpha_{Total-v}$ ) (see Table 1) indicated that the presence of clay colloids increased the attachment of virus

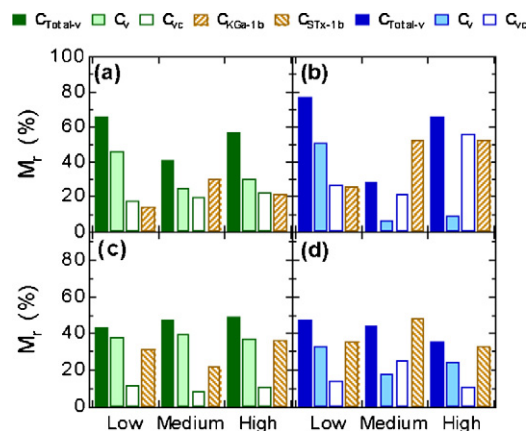


**Fig. 6.** Calculated  $M_r$  values based on  $C_{Total-v}$  (solid columns),  $C_v$  (filled columns),  $C_{vc}$  (open columns), and  $C_c$  (cross-shaded columns) for cotransport of: (a)  $\Phi X174$  with KGa-1b; (b) MS2 with KGa-1b; (c)  $\Phi X174$  with STX-1b; and (d) MS2 with STX-1b at low ( $U = 0.38$  cm/min), medium ( $U = 0.74$  cm/min) and high ( $U = 1.21$  cm/min) interstitial velocities.

**Table 2**  
Calculated DLVO and XDLVO interaction energy profile components, based on the sphere-plate model for glass beads.

	DLVO theory			XDLVO theory			
	$\Phi_{\max 1}$ ( $k_B T$ )	$\Phi_{\min 1}$ ( $k_B T$ )	$\Phi_{\min 2}$ ( $k_B T$ )	$\Phi_{\max 1}$ ( $k_B T$ )	$\Phi_{\min 1}$ ( $k_B T$ )	$\Phi_{\min 2}$ ( $k_B T$ )	$\Phi_{AB(h=h_0)}$ ( $\text{mJ}/\text{m}^2$ )
MS2	33.5	n/a <sup>a</sup>	0.00011	33.0	n/a <sup>a</sup>	0.00011	-0.711
$\Phi X174$	23.3	n/a <sup>a</sup>	0.00011	23.3	n/a <sup>a</sup>	0.00012	-0.004
KGa-1b	1072	163	0.00388	1053	53,711	0.00785	-42.2
STx-1b	973.5	1438	0.00567	973.4	3604	0.00115	-1.21

<sup>a</sup>  $\Phi_{\min 1}$  does not exist.

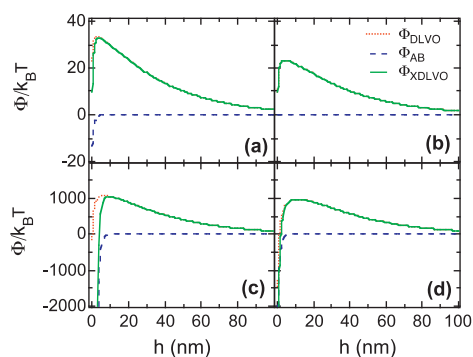


**Fig. 7.** Predicted sphere-plate  $\Phi_{DLVO}$ ,  $\Phi_{AB}$ , and  $\Phi_{XDLVO}$  interaction energy profiles for: (a) MS2 and glass beads, (b)  $\Phi X174$  and glass beads, (c) KGa-1b and glass beads, and (d) STx-1b and glass beads, as a function of separation distance (here  $\text{pH} = 7$ ,  $I_s = 10^{-4}$  M).

onto glass beads and clay colloids. In all cases examined,  $\alpha_v$  values decreased with decreasing  $U$ . According to the CFT, decreasing  $U$  increases the number of collisions of colloids with collectors and consequently increases colloid retention in porous media [70–72]. Note that the CFT assumes that the column packing is clean, and that deposited colloids do not affect the rate of colloid removal [48]. If a collector becomes partly blocked by the presence of attached viruses and clay colloids, the overall  $\alpha_{\text{Total-v}}$  and  $\alpha_v$  may either increase or decrease when additional viruses and clay colloids are added, depending on whether clay–clay, virus–virus and clay–virus attachment is favorable or unfavorable [28].

Moreover, the higher  $\alpha_v$  values observed for MS2 in the presence of both KGa-1b and STx-1b could be attributed to the greater affinity of MS2 for both clay particles [40]. Worthy to note is that, in agreement with the experimental results of this study, Chrysikopoulos and Syngouna [40] reported that  $\Phi_{AB(h=h_0)}$  values were more negative for MS2 than  $\Phi X174$  interactions with the two clays examined.

#### 4.3. DLVO and XDLVO calculations

Fig. 7 illustrates the estimated  $\Phi_{DLVO}$ ,  $\Phi_{AB}$ , and  $\Phi_{XDLVO}$  interaction energy profiles calculated for the case of sphere-plate approximation for virus-glass beads and clay-glass beads interactions under the experimental conditions of this study ( $\text{pH} = 7$ ,  $I_s = 10^{-4}$  M). The estimated  $\Phi_{\max 1}$ ,  $\Phi_{\min 1}$ ,  $\Phi_{\min 2}$  values are listed in Table 2 together with the various Lewis acid–base free energy of interaction values. Using classical DLVO theory, the results revealed that the experimental conditions were unfavorable to deposition. In the present study, MS2 ( $-40.4 \pm 3.7$  mV) was more negatively charged than  $\Phi X174$  ( $-31.8 \pm 1.3$  mV) at pH 7 (see Table 2), and thus the repulsive electrostatic force between MS2 and glass beads (see Fig. 7a) was larger than that between  $\Phi X174$  and glass beads (see Fig. 7b). However, greater amounts of adsorption were observed for MS2 than  $\Phi X174$  at pH 7. This implied that for viral adsorption on glass beads, non-electrostatic forces (e.g. hydrophobic) may be more important than electrostatic forces.

The non-electrostatic forces were also found to be important for bacteria attachment onto kaolinite and montmorillonite [38], virus attachment onto silica [73], and bacteriophage attachment onto hectorite, saponite, and kaolinite [74]. XDLVO theory suggested that there are stronger hydrophobic interactions between MS2 and glass beads ( $\Phi_{AB(h=h_0)} = -0.711$   $\text{mJ}/\text{m}^2$ ) than  $\Phi X174$  and glass beads ( $\Phi_{AB(h=h_0)} = -0.004$   $\text{mJ}/\text{m}^2$ ). Clearly, the  $\Phi_{AB}$  interaction energy for the viruses did not significantly affect  $\Phi_{XDLVO}$  profiles, and virus attachment onto glass beads. Similar  $\Phi_{DLVO}$  profiles were constructed for the interaction between clays with glass beads (Fig. 7c and d). However, for clay colloids the  $\Phi_{XDLVO}$  profiles exhibited a deeper  $\Phi_{\min 1}$  compared to that of  $\Phi_{DLVO}$  profiles, suggesting that Lewis acid–base interactions played an important role in the total clay colloid-glass bead interaction energy, and that they worked to the advantage of clay colloid attachment onto glass beads, with more hydrophobic interaction between KGa-1b and glass beads ( $\Phi_{AB(h=h_0)} = -42.2$   $\text{mJ}/\text{m}^2$ ) than STx-1b and glass beads ( $\Phi_{AB(h=h_0)} = -1.21$   $\text{mJ}/\text{m}^2$ ) (see Table 2). Worthy to note is that the cotransport results of this study are in agreement with those reported by Chrysikopoulos and Syngouna [40], who estimated higher values of the Freundlich parameter ( $K_f$ ) for KGa-1b than STx-1b, indicating stronger affinity of both viruses for KGa-1b. Viral adsorption onto clays is often proportional to the SSA and CEC of the clay minerals. However, a large portion of the SSA for STx-1b is inner surface area, which is not accessible for viral adsorption. The viral affinity for clay minerals is also supported by the XDLVO theory. The previously calculated Lewis acid–base free energy values of viral adsorption onto minerals suggested more favorable virus adsorption onto KGa-1b than by STx-1b, and stronger hydrophobic interaction between MS2 and clay minerals than  $\Phi X174$  and clay minerals [40].

## 5. Conclusions

In this study, we have examined the individual effects of two major parameters (presence/absence of clay colloids, and pore water velocity) that influence virus and colloid cotransport. Under field conditions the transport of viruses is more complex and is influenced by various physicochemical parameters. However, we expect that pore water velocity has the greatest relative impact on virus-colloid cotransport. Please note that transport of a suspended particle may be enhanced or retarded compared to the tracer, while virus transport may be facilitated or hindered in the presence of suspended clay particles compared to the case where suspended particles are absent. The results of this study indicated that the mass recovery of viruses and clay colloids decrease with decreasing pore water velocity; whereas, for the cotransport experiments no clear trend was observed. Moreover, in the most cases examined, the  $M_r$  values based on  $C_{\text{Total-v}}$  and  $C_{vc}$  of both viruses in the presence of STx-1b were lower than those in the presence of KGa-1b. In both transport and cotransport experiments, MS2 and  $\Phi X174$  transport was retarded ( $M_{1(i)}/M_{1(t)} < 1$ ) compared to the conservative tracer only at the highest pore water velocity tested. For the other two velocities both viruses were slightly enhanced

( $M_{1(i)}/M_{1(t)} > 1$ ) compared to the tracer. At the lower pore water velocities, the presence of clay colloids facilitated the transport of  $\Phi X174$  ( $M_{1(i)}/M_{1(t)}$  of  $C_{Vc} > M_{1(i)}/M_{1(t)}$  of  $C_{Total-v} > 1$ ) with the exception of  $U = 0.74$  cm/min in the presence of KGa-1b, while hindered the transport of MS2 ( $M_{1(i)}/M_{1(t)}$  of  $C_{Total-v} > M_{1(i)}/M_{1(t)}$  of  $C_{Vc} > 1$ ). At the highest pore water velocity clay colloids hindered the transport of both viruses ( $M_{1(i)}/M_{1(t)}$  of  $C_{Vc} < M_{1(i)}/M_{1(t)}$  of  $C_{Total-v} < M_{1(i)}/M_{1(t)}$  of  $C_v < 1$ ). Moreover, the cotransport results revealed a greater hydrophobic interaction-mediated attachment of both MS2 and  $\Phi X174$  onto KGa-1b than STx-1b. Also, MS2 exhibited greater affinity than  $\Phi X174$  for both clays. Lewis acid–base interactions did not significantly affect virus attachment onto glass beads, but they played an important role in the total clay colloid–glass bead interaction energy, and worked to the advantage of clay colloid attachment onto the glass beads. Note that although and inactivation rate of viruses in the laboratory-scale column experiments of this study were found to be relatively negligible due to the short residence times, certainly, this may not be the case for biocolloid transport at the field-scale where the detachment rates and inactivation constants of suspended ( $C_v$ ) and attached ( $C_v^*$ ,  $C_{Vc}$ ,  $C_{Vc}^*$ ) viruses could be significant.

### Acknowledgments

This research has been co-financed by the European Union (European Social Fund-ESF) and Greek National Funds through the Operational program “Education and Lifelong Learning” under the action Aristeia I (Code No. 1185).

### References

- [1] R.W. Buddemeier, J.R. Hunt, Transport of colloidal contaminants in groundwater: radionuclide migration at the Nevada test site, *Appl. Geochem.* 3 (1988) 535–548.
- [2] A. Abdel-Salam, C.V. Chrysikopoulos, Analysis of a model for contaminant transport in fractured media in the presence of colloids, *J. Hydrol.* 165 (1995) 261–281.
- [3] M.E. Tatalovich, K.Y. Lee, C.V. Chrysikopoulos, Modeling the transport of contaminants originating from the dissolution of DNAPL pools in aquifers in the presence of dissolved humic substances, *Transport Porous Med.* 38 (1/2) (2000) 93–115.
- [4] M. Ibaraki, E.A. Sudicky, Colloid-facilitated contaminant transport in discretely fractured porous media: 1. Numerical formulation and sensitivity analysis, *Water Resour. Res.* 31 (12) (1995) 2945–2960.
- [5] D. Grolimund, M. Borkovec, K. Barmettler, H. Stichler, Colloid-facilitated transport of strongly sorbing contaminants in natural porous media: a laboratory column study, *Environ. Sci. Technol.* 30 (1996) 3118–3123.
- [6] J.E. Sifers, G.M. Hornberger, The role of colloidal kaolinite in the transport of cesium through laboratory sand columns, *Water Resour. Res.* 32 (1) (1996) 33–41.
- [7] R. Kretzschmar, M. Borkovec, D. Grolimund, M. Elimelech, Mobile subsurface colloids and their role in contaminant transport, *Adv. Agron.* 66 (1999) 121–194.
- [8] T.A. Camesano, K.M. Unice, B.E. Logan, Blocking and ripening of colloids in porous media and their implications for bacterial transport, *Colloids Surf. A* 160 (1999) 291–308.
- [9] D.K. Powelson, A.L. Mills, Transport of *Escherichia coli* in sand columns with constant and changing water contents, *J. Environ. Qual.* 30 (2001) 238–245.
- [10] S.B. Kim, S.J. Park, C.G. Lee, N.C. Choi, D.J. Kim, Bacteria transport through goethite-coated sand: Effects of solution pH and coated sand content, *Colloids Surf. B* 63 (2008) 236–242.
- [11] M. Tong, X. Li, C.N. Brow, W.P. Johnson, Detachment influenced transport of an adhesion-deficient bacterial strain within water-reactive porous media, *Environ. Sci. Technol.* 39 (2005) 2500–2508.
- [12] Y. Sim, C.V. Chrysikopoulos, Analytical models for one-dimensional virus transport in saturated porous media, *Water Resour. Res.* 31 (5) (1995) 1429–1437 (Correction, *Water Resour. Res.* 32(5), 1473, 1996).
- [13] Y. Sim, C.V. Chrysikopoulos, Three-dimensional analytical models for virus transport in saturated porous media, *Transport Porous Med.* 30 (1) (1998) 87–112.
- [14] Y. Sim, C.V. Chrysikopoulos, Virus transport in unsaturated porous media, *Water Resour. Res.* 36 (1) (2000) 173–179.
- [15] W.P. Johnson, P. Zhang, M.E. Fuller, T.D. Scheibe, B.J. Mailloux, T.C. Onstott, M.F. DeFlaun, S.S. Hubbard, J. Radtke, W.P. Kovacic, W. Holben, Ferruginous tracking of bacterial transport in the field at the Narrow Channel Focus Area, Oyster, VA, *Environ. Sci. Technol.* 35 (2001) 182–191.
- [16] A.A. Keller, S.S. Sirivithayapakorn, C.V. Chrysikopoulos, Early breakthrough of colloids and bacteriophage MS2 in a water-saturated sand column, *Water Resour. Res.* 40 (2004) W08304, <http://dx.doi.org/10.1029/2003WR002676>.
- [17] S.C. James, T.K. Bilezikjian, C.V. Chrysikopoulos, Contaminant transport in a fracture with spatially variable aperture in the presence of monodisperse and polydisperse colloids, *Stoch. Environ. Res. Risk Assess.* 19 (2005) 266–279.
- [18] R. Anders, C.V. Chrysikopoulos, Virus fate and transport during artificial recharge with recycled water, *Water Resour. Res.* 41 (2005) W10415, <http://dx.doi.org/10.1029/2004WR003419>.
- [19] R. Anders, C.V. Chrysikopoulos, Transport of viruses through saturated and unsaturated columns packed with sand, *Transport Porous Med.* 76 (2009) 121–138.
- [20] S. Torkzaban, S.S. Tazehkand, S.L. Walker, S.A. Bradford, Transport and fate of bacteria in porous media: coupled effects of chemical conditions and pore space geometry, *Water Resour. Res.* 44 (2008) W04403, doi:04410.01029/02007WR006541.
- [21] C. Masciopinto, R. La Mantia, C.V. Chrysikopoulos, Fate and transport of pathogens in a fractured aquifer in the Salento area, Italy, *Water Resour. Res.* 44 (2008) 743, W01404, doi:10.1029/2006WR005643.
- [22] C.V. Chrysikopoulos, C. Masciopinto, R. La Mantia, I.D. Manariotis, Removal of biocolloids suspended in reclaimed wastewater by injection in a fractured aquifer model, *Environ. Sci. Technol.* 44 (3) (2010) 971–977.
- [23] M.Y. Corapcioglu, S. Kim, Modeling facilitated contaminant transport by mobile bacteria, *Water Resour. Res.* 31 (11) (1995) 2639–2647.
- [24] A. Abdel-Salam, C.V. Chrysikopoulos, Modeling of colloid and colloid-facilitated contaminant transport in a 2-dimensional fracture with spatially-variable aperture, *Transport Porous Med.* 20 (1995) 197–221.
- [25] Y. Jin, E. Pratt, M. Yates, Effect of mineral colloids on virus transport through saturated sand columns, *J. Environ. Qual.* 29 (2000) 532–540.
- [26] J. Simunek, C.M. He, L.P. Pang, S.A. Bradford, Colloid-facilitated solute transport in variably saturated porous media: numerical model and experimental verification, *Vadose Zone J.* 5 (2006) 1035–1047.
- [27] H.M. Bekhit, M.A. El-Kordy, A.E. Hassan, Contaminant transport in groundwater in the presence of colloids and bacteria: model development and verification, *J. Contam. Hydrol.* 108 (2009) 152–167.
- [28] G.E. Walshe, L. Pang, M. Flury, M.E. Close, M. Flintoft, Effects of pH, ionic strength, dissolved organic matter, and flow rate on the cotransport of MS2 bacteriophages with kaolinite in gravel aquifer media, *Water Res.* 44 (2010) 1255–1269.
- [29] Y. Jin, M. Flury, Fate and transport of viruses in porous media, *Adv. Agronomy* 77 (2002) 39–102.
- [30] J.F. Schjiven, W. Hoogenboezem, S.M. Hassanizadeh, Modelling removal of bacteriophages MS2 and PRD1 by dune recharge at Castricum, Netherlands, *Water Resour. Res.* 35 (1999) 1101–1111.
- [31] M.D. Sobsey, R.M. Hall, R.L. Hazard, Comparative reduction of hepatitis A virus, enterovirus and coliphage MS2 in miniature soil columns, *Water Sci. Technol.* 31 (1995) 203–209.
- [32] D.C. DeBorde, W.W. Wossener, Q.T. Kiley, P. Ball, Rapid transport of viruses in a floodplain aquifer, *Water Res.* 33 (1999) 2229–2238.
- [33] M.H. Adams, Bacteriophages, Interscience, New York, NY, 1959, pp. 450–454.
- [34] V.I. Syngouna, C.V. Chrysikopoulos, Interaction between viruses and clays in static and dynamic batch systems, *Environ. Sci. Technol.* 44 (2010) 4539–4544.
- [35] V.I. Syngouna, C.V. Chrysikopoulos, Transport of biocolloids in water saturated columns packed with sand: effect of grain size and pore water velocity, *J. Contam. Hydrol.* 126 (2011) 301–314.
- [36] J.A. Snowdon, D.O. Cliver, C.J. Hurst, Coliphages as indicators of human enteric viruses in groundwater, *Crit. Rev. Environ. Control.* 19 (3) (1989) 231–249.
- [37] D. Jiang, Q. Huang, P. Cai, X. Rong, W. Chen, Adsorption of *Pseudomonas putida* on clay minerals and iron oxide, *Colloids Surf. B: Biointerfaces* 54 (2007) 217–221.
- [38] X. Rong, Q. Huang, X. He, H. Chen, P. Cai, W. Liang, Interaction of *Pseudomonas putida* with kaolinite and montmorillonite: a combination study by equilibrium adsorption, ITC, SEM and FTIR, *Colloids Surf. B: Biointerfaces* 64 (2008) 49–55.
- [39] I.A. Vasiliadou, C.V. Chrysikopoulos, Cotransport of *Pseudomonas putida* and kaolinite particles through water saturated porous media, *Water Resour. Res.* 47 (2011) W02543, <http://dx.doi.org/10.1029/2010WR009560>.
- [40] C.V. Chrysikopoulos, V.I. Syngouna, Attachment of bacteriophages MS2 and  $\Phi X174$  onto kaolinite and montmorillonite: extended DLVO interactions, *Colloids Surf. B: Biointerfaces* 92 (2012) 74–83.
- [41] C.V. Chrysikopoulos, A.F. Aravantinou, Virus inactivation in the presence of quartz sand under static and dynamic batch conditions at different temperatures, *J. Hazard. Mater.* 233/234 (2012) 148–157.
- [42] R.J. Pruett, H.L. Webb, Sampling and analysis of KGa-1b well-crystallized kaolin source clay, *Clays Clay Miner.* 41 (4) (1993) 514–519.
- [43] H. Van Olphen, J.J. Fripiat, Data Handbook for Clay Minerals and Other Non-metallic Minerals, Pergamon Press, Oxford, England, 1979, 346pp.
- [44] R.L. Sanders, N.M. Washton, K.T. Mueller, Measurement of the reactive surface area of clay minerals using solid-state NMR studies of a probe molecule, *J. Phys. Chem. C* 114 (12) (2010) 5491–5498.
- [45] I.A. Vasiliadou, D. Papoulis, C.V. Chrysikopoulos, D. Panagiotaras, E. Karakosta, M. Fardis, G. Papavassiliou, Attachment of *Pseudomonas putida* onto differently structured kaolinite minerals: a combined ATR-FTIR and  $^1H$  NMR study, *Colloids Surf. B: Biointerfaces* 84 (2) (2011) 354–359, <http://dx.doi.org/10.1016/j.colsurfb.2011.01.026>.
- [46] J.F.L. Duval, H. Ohshima, Electrophoresis of diffuse soft particles, *Langmuir* 22 (2006) 3533–3546.

- [47] J.F.L. Duval, F. Gaboriaud, Progress in electrohydrodynamics of soft microbial particle interphases, *Curr. Opin. Colloid Interface Sci.* 15 (2010) 184–195.
- [48] C.V. Chrysikopoulos, Artificial tracers for geothermal reservoir studies, *Environ. Geol.* 22 (1993) 60–70.
- [49] R. Rajagopalan, C. Tien, Trajectory analysis of deep-bed filtration with the sphere-in-cell porous media model, *AIChE J.* 22 (1976) 523–533.
- [50] S.C. James, C.V. Chrysikopoulos, Monodisperse and polydisperse colloid transport in water-saturated fractures with various orientations: gravity effects, *Adv. Water Resour.* 34 (10) (2011) 1249–1255.
- [51] N. Tufenkji, M. Elimelech, Correlation equation for predicting single-collector efficiency in physicochemical filtration in saturated porous media, *Environ. Sci. Technol.* 38 (2004) 529–536.
- [52] J.P. Murray, G.A. Parks in, M.C. Kavanaugh, J.O. Leckie (Eds.), *Particulates in water: characterization, fate, effects and removal*, *Adv. Chem. Ser.*, vol. 189, American Chemical Society, Washington, DC, 1978.
- [53] H. Feng, Z. Yu, P.K. Chu, Ion implantation of organisms, *Mater. Sci. Eng. Rep.* 54 (2006) 49–120.
- [54] R.A. Freeze, J.A. Cherry, *Groundwater*, Prentice-Hall, Englewood Cliffs, NJ, 1979, 604pp.
- [55] J.P. Loveland, J.N. Ryan, G.L. Amy, R.W. Harvey, The reversibility of virus attachment to mineral surfaces, *Colloids Surf. A: Physicochem. Eng. Aspects* 107 (1996) 205–221.
- [56] J. Bergendahl, D. Grasso, Prediction of colloid detachment in a model porous media: thermodynamics, *AIChE J.* 45 (1999) 475–484.
- [57] C.J. van Oss, *Interfacial Forces in Aqueous Media*, Marcel Dekker, New York, 1994.
- [58] C.J. van Oss, R.F. Giese, Role of the properties and structure of liquid water in colloidal and interracial systems, *J. Disper. Sci. Technol.* 25 (5) (2004) 631–655.
- [59] R.-H. Yoon, D.H. Flin, Y.I. Rabinovich, Hydrophobic interactions between dissimilar surfaces, *J. Colloid Interface Sci.* 185 (1997) 363–370.
- [60] C.J. van Oss, Acid–base interracial interactions in aqueous media, *Colloids Surf. A: Physicochem. Eng. Aspects* 78 (1993) 1–49.
- [61] R. Attinti, J. Wei, K. Kniel, J.T. Sims, Y. Jin, Virus' (MS2, ΦX174, and aichi) attachment on sand measured by atomic force microscopy and their transport through sand columns, *Environ. Sci. Technol.* 44 (2010) 2426–2432.
- [62] W. Wu, Baseline studies of the clay minerals society source clays: colloid and surface phenomena, *Clays Clay Miner.* 49 (5) (2001) 446–452.
- [63] N. Shahidzadeh-Bonn, A. Tournié, S. Bichon, P. Vié, S. Rodts, P. Faure, F. Bertrand, A. Azouni, Effect of wetting on the dynamics of drainage in porous media, *Transport Porous Med.* 56 (2004) 209–224.
- [64] Y. Jin, M.V. Yates, S.S. Thompson, W.A. Jury, Sorption interactions and survival of enteric viruses in soil materials, *Environ. Sci. Technol.* 31 (1997) 548–555.
- [65] I. McKissock, E.L. Walker, R.J. Gilkes, D.J. Carter, The influence of clay type on reduction of water repellency by applied clays: a review of some West Australian work, *J. Hydrol.* 231/232 (2000) 323–332.
- [66] A. Eynard, R. Lal, K.D. Wiebe, Water repellent soils, in: R. Lal (Ed.), *Encyclopedia of Soil Science*, 2nd ed., Taylor and Francis, New York, 2006, pp. 1860–1863.
- [67] C.J. Hurst, C.P. Gerba, I. Cech, Effects of environmental variables and soil characteristics on virus survival in soil, *Appl. Environ. Microb.* 40 (1980) 1067–1079.
- [68] C.P. Gerba, Applied and theoretical aspects of virus adsorption to surfaces, *Adv. Appl. Microbiol.* 30 (1984) 133–168.
- [69] M.V. Yates, S.R. Yates, Modeling microbial fate in the subsurface environment, *Crit. Rev. Environ. Control* 17 (4) (1988) 307–344.
- [70] T.A. Camesano, B.E. Logan, Influence of fluid velocity and cell concentration on the transport of motile and non-motile bacteria in porous media, *Environ. Sci. Technol.* 32 (11) (1998) 1699–1708.
- [71] N.C. Choi, D.J. Kim, S.B. Kim, Quantification of bacterial mass recovery as a function of pore-water velocity and ionic strength, *Res. Microbiol.* 158 (2007) 70–78.
- [72] L. Pang, Microbial removal rates in subsurface media estimated from published studies of field experiments and large intact soil cores, *J. Environ. Qual.* 38 (2009) 1531–1559.
- [73] K.S. Zerda, C.P. Gerba, K.C. Hou, S.M. Goyal, Adsorption of viruses to charge-modified silica, *Appl. Environ. Microbiol.* 49 (1985) 91–95.
- [74] S. Chattopadhyay, R.W. Puls, Adsorption of bacteriophages on clay minerals, *Environ. Sci. Technol.* 33 (1999) 3609–3614.